Analytical study of connection detailing role in seismic behaviour of SMRF: case of unequal beam depth

Peyman Shadmanheidari
East Tehran branch, Islamic Azad University, Tehran, Iran

R. Ahmady & B. H. Hashemi
Structural Research Centre ,International Institute of Earthquake Engineering and Seismology(IIEES), Tehran, Iran

H. Kayhani & Pouya Shadmanheidari
Science and Research Branch, Islamic Azad University, Tehran, Iran

SUMMARY:

This study is a part of ongoing research that considers the differences of seismic behaviour of Special Moment Resisting Frames (SMRF) with unequal beam depths, regarding connection type. There are some variations in connecting deep and shallow beams to the column. The studied connection detailing arrangements consist of continuity plate arrangements and connection type such as: flange plate, coverplate connections, and the haunch connection system on the shallow beam side. Six full-scale experiments were conducted in order to investigate the seismic behaviour for this special case, also companion analyses were conducted in order to consider the effects of the above-mentioned connection detailing arrangements on the analytical rupture indices. The results of experiments and analyses indicated that described connection detailing arrangements can achieve performance corresponding to AISC criteria (seismic provisions (**2005**)), and deep beam bottom flange fracture close to the end of reinforced-plate connections is dominant rupture mode for this special cases.

Keywords: SMRF, unequal beam depths, continuity plate arrangement

1. INTRODUCTION

Plate-reinforced connections are categorized as qualified connections in order to satisfy SMRF criteria (Fema-350 2000, FEMA 355-B 2000, FEMA, 355D 2000, and AISC 2000). The study on plate-reinforced has started in 80's by SAC joint venture and FEMA (1996). Engelhardt and Sabol(1997) performed twelve experiments with coverplate reinforced connections for exterior columns. Most of the investigated test specimens showed outstanding performance, and developed large plastic rotations. However, it should be noted that the provisions of FEMA-350(2000) emphasized that flange plates are superior to coverplates since the welding of a single plate, i.e. a flange plate connection, is more reliable than the welding of a combination of a beam flange and a coverplate.Kim et al. (2002) experimentally studied the cyclic behaviour of five coverplate and five flange plate reinforced connections for exterior columns. The results indicated that the nonlinear behaviour of these types of connections is better than that of the unreinforced connections. There was also no brittle failure in these experiments, and all the test specimens had maximum beam plastic rotations of between 2.3% and 3.9% radians. Chung-Che Chou and Chia-Ching (2007) studied the performance of steel reduced flange plate (RFP) moment connections for exterior columns, and evaluated the nonlinear behaviour of the RFP by means of nonlinear regression analysis. The results showed that there is outstanding performance for this type of connection, i.e. reduced flange plate (RFP) moment connections, compared to the flange plate connection (FP). B.H Hashemi R.A Jazany (2012) and (2010) studied the cyclic behaviour differences between cover plate and flange plate for unequal beam depth, they showed that the flange plate connections also has superiority over the coverplate but the role of continuity plate arrangement is important for this special cases.

Nakashima et al. (1998) performed 86 tests on full-scale beam-to-column connection sub-assemblies for exterior columns. The results of these tests showed that the ductility of the welded connections was affected by the type of run-off tab, but this result was not validated when the sub-assemblies were

subjected to dynamic loading. El-Tawil et al. (2000) investigated the effect of the yield-to-ultimate stress ratio on the inelastic behaviour of pre-Northridge connections. The results of these experiments indicated the detrimental effects of high yield-to-ultimate stress ratios on the inelastic behaviour of such connections. An experimental study by Dubina and Stratan (2002) indicated that double bevel groove welds show better performance and superior seismic behaviour to that of single bevel groove welds. Moreover, when the material strength was increased, the ductility of this type of connection decreased. Hopperstad et al. (2003) and Morquio and Reira (2004) have indicated that there is no significant effect of strain rate on steel elongation. Dexter and Melenderz (2000) performed an experimental study on forty small T-joint samples. The results of this study showed that high heat input welds and some detailing connections of the T-joint resulted in the triggering of the fracture, in spite of the high strain rate. The results also indicated that the lack of yielding in the through-thickness direction can be explained by the existence of triaxial constraint in the column flange material. Ricles et al. (2002) performed various experiments with the aim of improving the pre-Northridge detailing. This experimental work consisted of eleven full-scale specimens for exterior columns and thirty nine small-scale assemblies. The test results suggested that the use of weld metal with a minimum notch toughness of 27 J at -29◦C in conjunction with improved weld detailing including the removal of weld back bars could prevent weld line fracture and reduced fracture potential in welded moment connection frames. Anderson et al. (2002) showed that the application of weld overlays to the small size specimens resulted in a significant improvement in their cyclic performance. The plastic rotation capacity of both specimens was either close to or exceeded 3%. The application of weld overlays to the moment connection of the intermediate size specimen also improved the rotation capacity. Variations in the material properties lead to inaccurate prediction of weakness zones, and the use of weld filler metal with low notch toughness may result in premature failures of welds and improper geometry of the connection could intensify the high triaxial stress conditions and limit the uni-axial yield potential close to the connection (Bonowitz 1995, Fisher et al 1996 and 1997). Many of these brittle fractures were propagated into the column base metal, including fractures that appeared to scoop out some of the column material, referred to as mouse-ears or divots(Kaufmann et al 1996 and 1997). From the fractography that has been performed on these fractures (Ojdrovic Zarghamee(1997)), the primary cause of the fractures was identified as low-toughness weld filler metal combined with the existence of backing-bar notches and lack of fusion defects at the weld root.

2. TEST SPECIMENS DESCRIPTIONS

In order to develop the understanding of SMRF seismic behavior with unequal beam depth, six experiments were conducted in full scale for interior column and unequal beam depth. To simulate the actual conditions of SMRF, six sub-assemblages with different connection detailing arrangements were considered (Hashemi and Ahmadi 2010 and 2012). The sub-assemblages were full-scale simulations of an SMRF. They were extracted from the frame assuming that the inflection point is at the mid-point of all the elements. The experimental program at IIEES (International Institute of Earthquake Engineering and Seismology) was performed to provide a comprehensive understanding of the seismic behavior of the SMRF with unequal beam depths. Figure 1 shows the test setup including reaction supports and out of plane buckling supports for the beams. The bottom ends of the column were pinned to the strong floor of the laboratory, and out-of-plane buckling prevention devices were installed at the mid-point of the beam spans. Two hydraulic actuators for simulation of the seismic load were applied on the specimens' beam tips which were fixed on the strong floor of the structural laboratories. One of hydraulic actuators was capable of applying loads up to 1000 KN and a stroke of up to ±150 mm for the deep beam, and another was capable of applying loads up to 500 KN and a stroke of up to ±150 mm for the shallow beam. The storey drift angle of 0.01 radians corresponded to the displacement of 20 mm at a hinge of hydraulic jack. Figure 2 shows the displacement load pattern which originated from the AISC seismic provisions load pattern (AISC 2005). This load pattern was applied for the beams' tip in reverse direction and in plane situation to simulate seismic excitation.

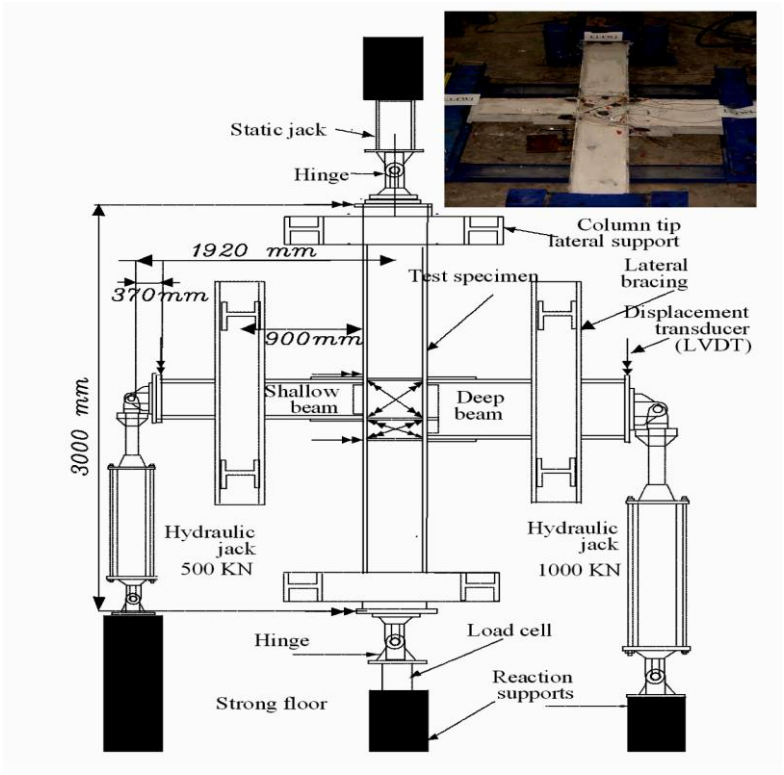

Figure 1. Schematic view of test set up

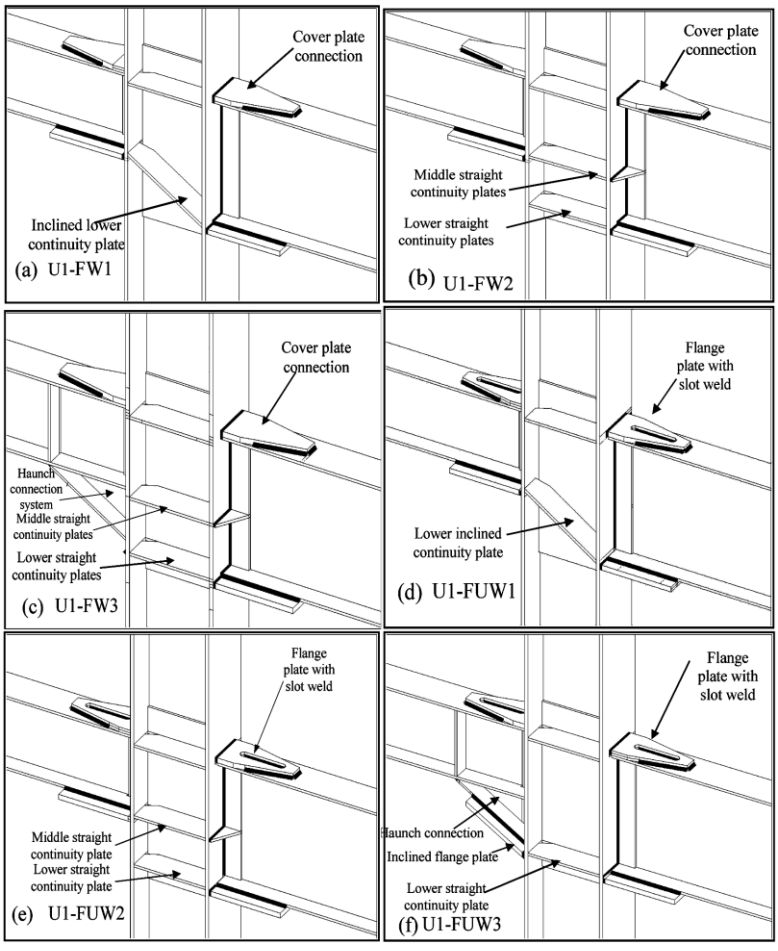

Figure 2. Connection detailing arrangements for six specimens (Hashemi and Ahmadi 2010 and 2012)

Test specimen U1-FUW1 consisted of a trapezoidal top flange plate connection and a rectangular bottom flange plate at the shallow beam (beam 30) and deep beam (beam 50) with an inclined lower continuity plate, which was fitted to meet the beams' bottom flanges as shown in Figure 2 (Hashemi and Ahmadi 2010 and 2012). To provide enough weld line in accordance with FEMA-350 (2000), a slot weld was used for both the top and bottom flange plates. For the bottom flange plate, the slot welding was performed in overhead positions in the experiment similar to actual constructional conditions. Test specimen U1-FW1 was similar to U1-FUW1, but a coverplate connection was used for this test specimen instead of a flange plate, as shown in Figure 3(a). Test specimens U1-FUW2 and U1-FW2 were similar to U1-FUW1 and U1-FW1, respectively, except for the lower straight continuity plate and middle continuity plates which were used for these test specimens instead of inclined continuity plates, as shown in Figure 3(e) and Figure 3(b), respectively. As shown in Figure 3(c), test specimen U1-FW3 consisted of a coverplate connection on the deep beam side, including a top and bottom coverplate connection, whereas for the shallow beam, a top coverplate connection was used and a bottom coverplate was not used for the bottom flange (Hashemi and Ahmadi 2010 and 2012).

Table 1. Data about the investigated test specimens(Hashemi and Ahmadi(2010)

Specimen name	Beam	Column flanges	Column web	Doubler plates	WELD (6013,4 mm)	Lower continuity plate arrangement and number of lower continuity plates	Connection type
	F_y F_U	F_y F_U	F_y F_U	F_y F_U	F_y F_U		
U1-FUW1	230.3 373.8	269.2 390.1	245 373.8	260.5 385	460 522	Inclined(1)	Flange plate
U1-FUW2						Straight(2)	Flange plate
U1-FUW3						Straight(1)	Flange plate
U1-FW1						Inclined(1)	Coverplate
U1-FW2						Straight(2)	Coverplate
U1-FW3						Straight(2)	Coverplate

Unit: MPa

The test specimen U1-FUW3 consisted of a flange plate connection with a slot weld on the deep beam side, including the top and bottom flange plate connection. The assemblage of the shallow beam and haunch system is connected to the column flange by a top flange plate and an inclined bottom flange plate, which is connected to the haunch flange by a fillet weld line as shown in Figure 3(f) (Hashemi and Ahmadi 2010 and 2012). The advantages of using an inclined flange plate are: (1) it is possible to assemble the shallow beam and haunch system away from the column erection site and (2) the welding of shallow beam bottom flange to haunch web connection can be performed in the horizontal or flat position.

3. EXPERIMENTAL RESULTS

3.1. Test Specimen U1-FUW1

Test specimen U1-FUW1 underwent elastic response in the first 20 cycles (the 20th cycle corresponded to storey drift angle of 1.0 %) of loading. Based on the strain gauge data fixed to the PZ, the PZ yielding started at the corners which was close to the shallow beam at the 21st cycle (at 1% drift), then the deep beam yielded away from the column flange nearly at the 22nd cycle (at 1.5% drift). Local deep beam bottom flange buckling occurred at a 4% and 5% storey drift ratio and yet no local buckling of the web was observed at the deep and shallow beam plastic hinge region. Test specimen U1-FUW1 underwent severe inelastic behavior at cycle 34 which corresponds to the storey drift angle of 0.06 radians and the local bucking at deep beam web close to the bottom flange and deep beam bottom flange occurred. Table 1 shows test results and cause of test termination for each test specimen.

3.2. Test Specimen U1-FUW2

During the first 21 cycles (the 21st cycle corresponded to storey drift angle of 1.0 %), the behaviour of test specimen U1-FUW2 was also in the elastic range. The PZ yielding started at the 23rd cycle at the corners which were close to the deep beam (at 1.5% drift), but deep beam yielding started earlier, and the deep beam bottom flange of test specimen U1-FUW2 experienced local buckling at storey drift angle of 0.04 radians. This phenomenon was coincident with deep beam web buckling and shallow beam bottom flange buckling at a storey drift angle of 0.05 radians. Deep beam flange fracture close to the end of the flange plate occurred at a storey drift angle of 0.05 radians and the test was terminated.

3.3. Test Specimen U1-FUW3

Test specimen U1-FUW3 also showed elastic behaviour during the first 22 cycles (the 22nd cycle corresponded to storey drift angle of 1.5 %). Regarding strain gauge data, deep beam, shallow beam and PZ underwent nonlinear behavior at the 23rd cycle (with 1.5% drift). The substantial inelastic deformation took place beyond the end of the flange plate connections as shown in Figure 8 at the 34th cycle which was equal to a storey drift angle of 0.06 radians. During the test, no significant flange buckling and web local buckling was observed; hence, the degradation of strength and stiffness are not observed in the cyclic response of deep beam in this specimen as shown in Figure 9. Moreover, the large whitewashed area of the deep beam, shallow beam and the entire area of PZ flaked off. In order to prevent apparatus damage, the test was terminated at a storey drift angle of 0.06 radians. The crack initiation or rupture was not observed in all elements of these specimens.

3.4. Test Specimen U1-FW1

Test specimen U1-FW1 experienced elastic response within the first 21 cycles (the 21st cycle corresponded to storey drift angle of 1.0 %). Similar to specimen U1-FUW1, the PZ of this specimen yielded earlier than the beams. The specimen U1-FW1 underwent inelastic behavior, but there were not significant web and flange buckling at a storey drift angle of 0.04 and 0.05 radians corresponding to the 30th and 32nd cycles. Deep beam bottom flange rupture suddenly occurred at a storey drift angle of 0.05 radians, and the test was terminated.

3.5. Test Specimen U1-FW2

Specimen U1-FW2 indicated elastic behavior within the first 21 cycles (the 21st cycle corresponded to storey drift angle of 1.0 %) and the deep beam started to yield at the 22nd cycle (at 1.5% drift) and the PZ upper segment yielded at the 23rd cycle. The specimen underwent inelastic behavior without any significant buckling at beam flanges and web, and there is no degradation in the hysteresis behavior of the deep beam as shown Figure 9. The specimen failed due to deep beam bottom flange fracture at a storey drift angle of 0.05 radians, and the test was terminated.

3.6. Test Specimen U1-FW3

Test specimen U1-FW3 showed the worst response regarding the value of storey drift angle than all other specimens, resulting in poor performance. This specimen experienced elastic behavior within the first 21 cycles (the 21st cycle corresponded to storey drift angle of 1.0 %) and the deep beam started to yield at the 22nd cycle (at 1.5 % drift) and then PZ yielded one cycle later. The deep beam bottom flange buckling happened at a storey drift angle of 0.03 radians. The specimen underwent inelastic behavior at a storey drift angle of 0.04 radians and the deep beam bottom flange fractured at a storey drift angle of 0.04 .

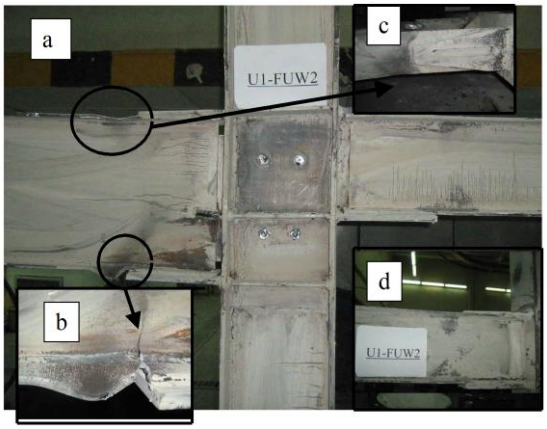

Figure 3. (a) View of specimen U1-FUW2 erected after the experiment and flaking of whitewashed area at deep and shallow beam and PZ upper segment (rear view) (b) deep beam bottom flange fracture (rear view) (c) deep beam top yielding area (top view) (d) flaking of whitewashed area at the shallow beam (front view)

Table 2. Experimental results

Specimen name	Drift angle (radians)	Shallow beam side Plastic rotation max	Shallow beam side Plastic rotation min	Deep beam side Plastic rotation max	Deep beam side Plastic rotation min	Test termination cause
U1-FW1	0.05	0.038	-0.036	0.039	-0.036	Deep beam bottom Flange fracture
U1-FW2	0.05	0.041	-0.038	0.045	-0.043	Deep beam bottom Flangefracture
U1-FW3	0.04	0.024	-0.028	0.027	-0.037	Deep beam bottom Flange fracture
U1-FUW1	0.06	0.043	-0.044	0.044	-0.046	Without any failure up To .06 radians
U1-FUW2	0.05	0.034	-0.035	0.040	-0.038	Deep beam bottom Flange fracture
U1-FUW3	0.06	0.042	-0.042	0.046	-0.046	Without any failure up To .06 radians

4. EXPERIMENTAL RESULTS

To evaluate the accuracy of finite element modeling approach, six finite element models are created according to actual test. From figures 4, it can be seen that the cyclic results obtained from the finite element models have good agreement with test data. Differences between the numerical simulation and test result may be the result of several causes like numerical modeling simplification, test specimen defect or residual stress also the differences between the test data and the numerical models grow in nonlinear portion of curve. It can be mentioned that the material properties, which are used in FE, are from average, but in reality steel is not a homogenous material and amount of every coupon test result could affect the actual result. Fig 5(a) shows analytical model of the test specimen U1-FW2 and Fig 5(b) shows equivalent plastic stress for this analytical model.

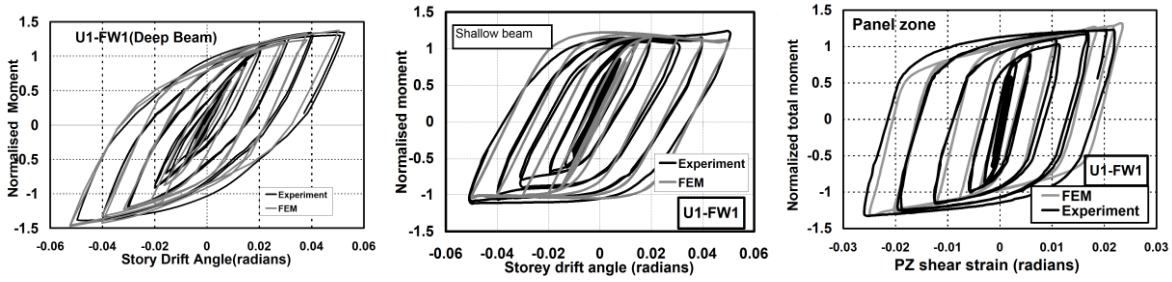

Figure 4. Plot of analytical and cyclic response of the deep beam, shallow beam and panel zone for the test specimen U1-FW1

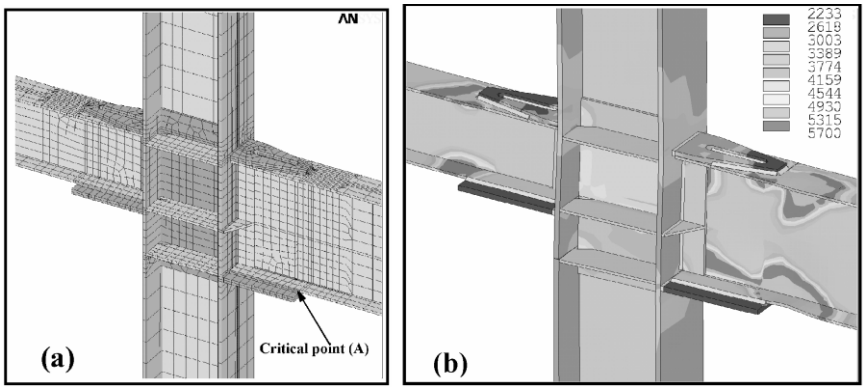

Figure 5.(a) Analytical model of the test specimen U1-FUW2 AND the critical points (b)Plot of equivalent plastic distribution for the test specimen U1-FUW2

5. ANALYTICAL EVALUATION OF DEEP BEAM BOTTOM FLANGE FRACTURE

The ratio of the equivalent plastic strain to the yield strain, which appears in the numerator of Eq. (1), is called the equivalent plastic strain index (PEEQ). This index is a measure of the local inelastic strain demand, and is also useful in evaluating and comparing different configurations (Hashemi and Ahmadi(2010)). The PEEQ index can be computed from the following expression:

$$PEEQ = \frac{\sqrt{\frac{2}{3}\varepsilon_{ij}^{p}.\varepsilon_{ij}^{p}}}{\varepsilon_{y}} \qquad [1]$$

where ε_{ij}^{p} are the plastic strain components.

Values of the triaxiality ratio and PEEQ indices were computed for the different continuity plate arrangements and different investigated corner clip lengths, thus providing an additional means to compare the different cases. For all the models, the critical point was located at the intersection of the doubler plates' fillet weld line and the doublerplates, close to the shallow beam's bottom coverplate (see point "A" in Figure 5(a)). Figures 5(a), also, show the corresponding FE models of test specimens U1-FW2

The equivalent plastic strain (ε_{eqv}^{pl}), calculated from the inelastic analysis, can be used as an indicator of initial cracking in the analytical models. In the analysis, ε_{eqv}^{pl} is based on the plastic strain component and on the general Von-Mises equation:

$$\varepsilon_{eqv}^{pl} = \frac{1}{\sqrt{2}(1+\upsilon')}\left[\left(\varepsilon_{x}^{pl}-\varepsilon_{y}^{pl}\right)^{2}+\left(\varepsilon_{y}^{pl}-\varepsilon_{z}^{pl}\right)^{2}+\left(\varepsilon_{z}^{pl}-\varepsilon_{z}^{pl}\right)^{2}+\frac{2}{3}\left(\gamma_{xy}^{pl^{2}}+\gamma_{yz}^{pl^{2}}+\gamma_{zx}^{pl^{2}}\right)\right]^{\frac{1}{2}} \qquad [2]$$

where ε_{eqv}^{pl}, is the equivalent plastic strain , ε_{y}^{pl} , γ_{xy}^{pl} etc. are the appropriate components of the plastic strain and υ' is the effective Poisson's ratio .Hancock and Mackenzie(1976), proposed a simplified model . Some studies by El-Tawil et al. (1998) and Ferreira et al. (1998), have also suggested that crack initiation could be predicted with reasonable accuracy by defining a threshold value of ε_{eqv}^{pl} for the given stress-strain state. In the present study, values of ε_{eqv}^{pl} are approximately

similar and the variation of values of ε_{eqv}^{pl} happened at low tolerance and a definite range, thus a similar approach was adopted as part of this study. The initial cracking noted during the tests was ductile. This means that the cracks developed and lengthened prior to the final fracture. As a result, ε_{eqv}^{pl} was used as the primary indicator of fracture potential for the already mentioned critical points. These estimations, also, can be valid for equivalent plastic strain index (PEEQ).

Fig 6 shows values of equivalent plastic index versus story drift angle values for the mentioned connection detailing arrangement; The PEEQ value of the analytical model for test specimen U1-FW3 is larger than the values of the analytical models corresponding to the analytical models of the other test specimens. It reaches a value of 32 in the case of a storey drift angle of 0.06 radians. The corresponding value of the analytical model for the test specimen U1-FW3 reaches 15, at a storey drift angle of 0.04 radians, where deep beam bottom flange fracture occurred (Hashemi and Ahmadi 2012).

Also the smallest values of the equivalent plastic strain index demand occurred at the critical points of the analytical models corresponding to the test specimens U1-FUW1 and U1-FUW3. These values amounted to 11.5 and 12 at a storey drift angle of 0.06 radians respectively (Hashemi and Ahmadi 2012). These equivalent plastic strain index values can provide an explanation as to why such a rupture occurred in the deep beam bottom flange, i.e. excessive plastic strain accumulation for the analytical model of test specimen U1-FW3 at the critical points. The corresponding values for the analytical models of test specimens U1-FUW2, U1-FW1 and U1-FW2, at a storey drift angle of 0.05 radians, where deep beam bottom flange rupture occurred, amounted to 13.6, 15 and 15.3 respectively .

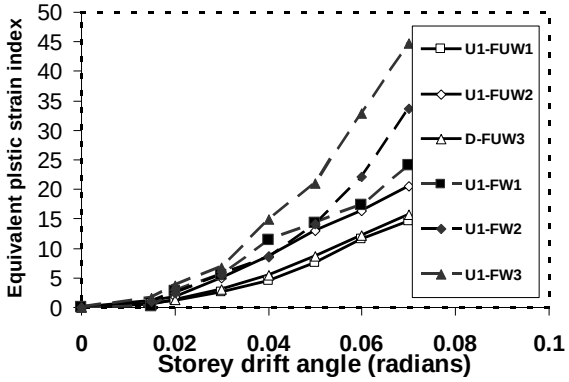

Figure 6. plot of equivalent plastic strain index for the analytical model of the test specimens

6. CONCLUSIONS

In this study, experiments of six full scale sub-assemblages with unequal beam depth were performed in order to represent the role of connection detailing arrangements in the seismic behavior and performance of welded connection moment resisting frame subjected to cyclic loading. The experiment revealed that deep beam bottom flange fracture could be premature failure mode before experiencing the storey drift angle of 0.06 radians for SMRF with unequal beam depth, the reasons may be due to asymmetric geometry of beams , PZ boundaries and connections around main column axis resulted in plastic strain accumulation at the intersection of deep beam bottom flange and plate-reinforced connection end i.e. coverplate and flange plate and less contribution of PZ shear deformation originating from connection type and continuity plate arrangement. Flange plate with haunch connection system, i.e. connection detailing arrangement of test specimen U1-FUW3, is the first alternative to eliminate the mentioned undesirable rupture mode; also connection detailing arrangement of test specimen U1-FUW1 could be second choice to exclude the mentioned rupture mode while other connection detailing arrangements ruptures before drift story angle of 0.06 radians.

References

AISC (2005). Seismic provisions for structural steel buildings. Chicago (IL), American institute of steel construction.

Anderson, JC, Duan, J., Xiao, Y, Maranian, P. (2002). Cyclic Testing of Moment Connections Upgraded with Weld Overlays. *J. Struct. Eng*. 128:4, 509-516.

Bonowitz D,. (1995).Surveys and assessment of damage to buildings affected by the Northridge earthquake of January 17, 1994. *Report SAC 95-06*, SAC Joint Venture, Richmond, California.

Chung-Che, Chou, Chia-Ching, Wu. (2007). Performance evaluation of steel reduced flange plate moment connections. *J Eq. Eng. Struct. Dyna.*, 36,2083–2097

Dexter RJ, Melenderz MI. (2000). Through–thickness properties of column flanges in welded moment connections.*J. Struct. Eng., ASCE*, 126:1, 24-31.

Dubina, D., Stratan, A. (2002). Behavior of welded connections of moment resisting frames beam to column joints. *Eng. Structs*, 24, 1431-40.

El-Tawil, S., Mikesell, T., Vidarsson, E., and Kunnath, S.K. 1998. Strength and ductility of FR welded-bolted connections. Report SAC/BD-**98/01** , SAC Joint Venture, Sacramento ,CA.

El-Tawil., S., Mikesell., T., Kunnath., SK. (2000). Effect of local details and yield ratio on behavior of FR steel connections. *J struct. Eng., ASCE*, 126:1, 79-87.

Engelhardt., MD., Sabol., TA. (1997). Reinforcing of steel moment connections with coverplates: Benefits and limitations. Engineering structures. *J Struct. Eng., ASCE*, 20(4-6), 510-20.

FEMA (2000). Recommended seismic design criteria for new steel moment frame building. Report no. FEMA 350, Federal Emergency Management Agency.

FEMA (2000). State of the art report on welding and inspection.Report no. FEMA-355B. Federal Emergency Management Agency.

FEMA. (1996).Experimental investigations of beam-column sub assemblages.Federal Emergency Management Agency Report *SAC-96-01*, Part 1, SAC Joint Venture, Sacramento (CA).

FEMA. (2000). State of the art report on connection performance.Report no. FEMA-355D. *Federal Emergency Management Agency*.

Ferreira, J., Castiglioni, C.A., Calado, L., Rosaria, and Agatino, M., (1998).Low cycle fatigue strength assessment of cruciform welded joints" Journal of Constructional Steel Research,**47**:3, 223–244.

Fisher JW, Dexter RJ, Kaufmann EJ.(1997). Fracture mechanics of welded structural steel connections. Report Number SAC 95-09, *FEMA-288*; 1997.

Fisher JW, Dexter, RJ. (1996). Fatigue and fracture. New York: McGraw-Hill, Chapter 8, LRFD Method.

Hancock, J.W., and Mackenzie, A.C. (1976).On the mechanisms of ductile failure in high strength steels subjected to multi-axial stress states. *J Mech. Phys. Solids*, 24: 147–169.

Hopperstad, OS.,Borvik, T.,Langseth., M,Labibies., K,Albertini, C. (2003). On the influence of stress triaxiality and strain rate on the behavior of a structural steel.Part I. Experiments, *Europe. J Mech. A/Solids*; 22,1-13.

Hosseini Hashemi B., Ahmady Jazany R. (2010).Experimental evaluation of cover plate and flange plate steel moment-resisting connections considering unequal beam depths. *journal of seismology and earthquake engineering*;12(3):89-106.

Hosseini Hashemi B., Ahmady Jazany R. (2012). Study of connection detailing on SMRF seismic behavior for unequal beam depths. *J. Constr. St. Res.*; 68:150–164.

Kaufmann, EJ, Fisher, JW, Di Julio, RM, Gross, JL. (1997). Failure analysis of welded steel moment frames damaged in the Northridge earthquake. NISTIR 5944, *National Institute of Standards and Technology*, Gaithersburg, Md.

Kaufmann, EJ, Fisher, JW.(1996). Fracture analysis of failed moment frame welded joints produced in full-scale laboratory tests and buildings damaged in the Northridge earthquake. Technical Report Number *SAC 95-08*, SAC Joint Venture, Richmond California.

Kim T, Whittakar AS, Gilani ASJ, Bertero VV, Takhirov SM. (2002). Cover-plate and flange-plate steel moment-resisting connections, *J Struct. Eng., ASCE*, 128:4, 474-82.

Morquio, A., Reira, JD. (2004). Size and strain rate effects in steel structures. *Eng. Struct*,26,669-79.

Nakishima, M., Tayetema, E., Morisako, K.,Suita, K. (1998).Full-Scale test of beam-column subassemblages having connection details of shop-welding type. *Structural Engineering Worldwide, Elsevier Science (CD-ROM),Paper Ref*. T158-7.

Ojdrovic, RP, Zarghamee, MS. (1997). A repair approach for fractured steel moment connections. Building to Last, Proceeding, Structural Congress XV, Reston, Va, Structural Engineering Institute, 596–601.

Ricles, JM., Fisher, JW. Kaufmann, EJ. (2002). Development of improved welded moment connections for earthquake-resistant design. *J Const. St. Res*., 58, 565-604.